Femtosecond laser-induced damage threshold of nematic liquid crystals at 1030 nm

Loïc Ramousse, Gilles Cheriaux, Cyrille Claudet, Aurélie Jullien

Femtosecond laser-induced damage threshold of nematic liquid crystals at 1030 nm

Loic Ramousse,[1, 2, *] Gilles Chériaux,[1] Cyrille Claudet,[1] and Aurélie Jullien[1]

[1] *Institut de Physique de Nice (INPHYNI), Université Côte d'Azur, CNRS, UMR 7010, 1361 route des Lucioles, 06560 Valbonne, France*
[2] *Fastlite, 165 route des Cistes, 06600 Antibes, France*

The laser-induced damage threshold (LIDT) of nematic liquid crystals is investigated in the femtosecond regime at $\simeq$ 1030 nm. The thickness and breakdown of freely-suspended thin films ($\simeq$ 100 nm) of different mixtures (MLC2073, MLC2132 and E7) is monitored in real time by spectral-domain interferometry. The duration of laser pulses was varied from 180 fs to 1.8 ps for repetition rates ranging from single-shot to 1 MHz. The dependence of the LIDT with pulse duration suggests a damage mechanism dominated by ionization mechanisms at low repetition rate and by linear absorption at high repetition rate. In the single-shot regime, LIDTs exceeding 1 J/cm^2 are found for the three investigated mixtures. The LIDT of polyvinyl alcohol (PVA) is also investigated by the same method.

INTRODUCTION

The large and tunable birefringence of nematic liquid-crystals (LCs) has been extensively studied and applied to the modulation and control of light [1–3]. For instance, LCs-based spatial light modulators (LC-SLMs) have been demonstrated as efficient adaptive optics for wavefront correction [4, 5], tunable phase-shifter for optical laser frequencies [6], tunable delay line in the microwave band [7], efficient phase-shifters for THz radiation [8]. If laser-induced damage threshold (LIDT) is not relevant for most uses of LCs, some laser applications do require LCs to operate at high peak fluence and/or high average power. Among scientific applications are the polarization control of energetic nanosecond pulses [9] and the direct manipulation of femtosecond pulse trains [10, 11]. In the context of industrial laser processing, and, in particular, of parallel writing and three-dimensional fabrication by ultrafast lasers, the power handling capabilities of LC-SLMs is a technical bottleneck [12]. The investigation of the LIDT of LCs at $\simeq$1 µm and the identification of the dominant damage mechanism is therefore of a key preliminary step to the adaptation and optimization of LC-SLMs to high peak/average power lasers.

For devices exploiting the electro-optic anisotropy of LCs, the electrode is known to be the LIDT limiting factor, whether made of Indium tin oxide, (ITO) [9, 13] or Gallium-Nitride (GaN) [14]. In order to improve resistance to laser-induced breakdown but also to extend the wavelength coverage of LC-SLMs, electric control can be abandoned in favor of optical addressing. Such electrode-free LC-SLMs have been achieved, for example, by inserting a photosensitive alignment layer [15] or by local thermo-optical control [16]. These works are an additional motivation to accurately determine the LIDT of the LCs themselves.

So far, several studies have been conducted with nanosecond pulsed near-infrared laser radiation [17, 18]. Recently, Kosc and co-authors reported on a systematic study to determine LIDT in thick nematic cells, for pulse duration ranging from 600 fs to 1.5 ns at different laser wavelengths (351 nm, 532 nm and 1053 nm) [19]. One of the conclusion of [19] is that saturated materials (i.e. featuring a higher bandgap energy) invariably exhibit higher LIDT that unsaturated ones. For the shortest pulse duration (600 fs) and in the single-shot regime at 1053 nm, the measured LIDT of biphenyl (E7) was approximately 0.7 J/cm^2. For shorter pulse durations, however, the LIDT remains to be determined.

In this paper, we investigate the LIDT on thin nematic liquid crystals films in the femtosecond regime at $\simeq$ 1030 nm. In order to remove the contributions of the confining substrates and of the anchoring layers, the measurements are performed on freely-suspended LC films with thicknesses of $\simeq$ 100 nm. Three different nematic mixtures are characterized: MLC2073, MLC2132 and E7. The optical breakdown is determined by a direct and *in situ* measurement of the optical thickness of the film via spectral-domain interferometry. Experimental dependencies of the LIDT with the pulse duration and repetition rate are assessed. We demonstrate that two regimes can be distinguished for LC breakdown. In the single-shot regime, breakdown seems dominated by the usual ionization processes in dielectrics and LIDT is found to be above 1 J/cm^2 for the three mixtures investigated here. In contrast, at high repetition rate, the breakdown seems dominated by thermal accumulation induced by a residual linear absorption. In both cases, these values complete the formerly reported study [19] and strengthen applications of nematics to intense and/or ultrashort light shaping.

DAMAGE SETUP AND DIAGNOSTIC

Experimental configuration

The laser source is a femtosecond diode-pumped Ytterbium laser (Pharos PH2-SP-1mJ, Light Conversion

* loic.ramousse@inphyni.cnrs.fr

) operating at a central wavelength of 1030 nm. The pulse duration can be tuned between (183±4) fs and 10 ps by adjusting the compression and is experimentally controlled with a scanning SH-FROG device (Frozzer, Fastlite) (Fig. 1b). The repetition rate of the laser can be varied from single shot to 1 MHz with a maximum pulse energy ranging from 1 mJ (in single shot) to 6 µJ (at 1 MHz). The pulse-to-pulse energy stability is 0.5% RMS.

The experimental setup is schematically depicted in Fig. 1a. The laser beam is linearly polarized and focused on the sample with a plano-convex lens (focal length f = 150 mm) at normal incidence. The profile and dimension of the laser beam on the focus plane is measured with a CCD camera (WinCamD-UCD12) and is plotted in Fig. 1c. The measured beam waist on the sample is (35±5) µm FWHM. The energy can be adjusted using both the attenuator integrated in the laser and a zero-order half wave plate combined with a linear polarizer. The sample is positioned on a motorised XYZ translation stage (Newport) with 1 µm precision. An endoscope enables visualization of the state of the sample in real time (Fig. 1e).

Thin nematic liquid crystal films

The fluid nature of LC mixtures usually requires confinement substrates and, most of the time, a polymer alignment layer. This multi-layered structure might contribute to incorrect LIDT measurements, either because of self-focusing in the substrates, and/or by interaction with the anchoring layer. To solve this issue, we have chosen to use self-hanging thin films of nematics as samples. Self-suspended smectic films have already been demonstrated to be reliable targets for laser-plasma interaction [20, 21]. In the present case, weak light diffusion from the film indicates that the nematic mesophase is not ordered and the forthcoming LIDT values have thus to be reported to an average molecular orientation.

For practical realization, we have followed the experimental procedure described in [20, 21]. A copper plate of 1.6 mm thickness with a 3 mm diameter hole is used as a support. A drop of liquid crystal is deposited next to the hole and spread above the aperture with a razor blade. A film is thus created and extends between the edges of the hole, as illustrated on the picture obtained with the endoscope on Fig. 1e. The films are first observed by optical microscopy (transmission mode, unpolarized light). A microscopic picture is shown in Fig. 1d: the film has a thin inner region that widens near the hole edge into a thicker meniscus. The inner thickness can be experimentally determined with spectral-domain interferometry (see below). Typical thickness varies between 50 nm and 400 nm, and is on average 100 nm, whatever the employed mixture (Fig. 2 b). Using freely-suspended films not only presents the advantage of simplifying the interaction picture but also offers a very convenient way to renew the LC, and therefore to adopt a probabilistic approach.

Three different mixtures of nematic LC are considered : MLC2073, MLC2132 and the widely employed E7 (all from Merck). Table I gathers their main optical properties. E7 and MLC2132 present a high optical birefringence together with positive dielectrical anisotropy, while MLC2073 has a smaller birefringence and negative dielectrical anisotropy. Their bandgap energy is comprised between 3.2 eV (E7 and MLC2132, unsaturated) and 4.3 eV (MLC2073, saturated). The laser wavelength (λ=1030 nm) falls well within the transparency range of all mixtures.

TABLE I. **LC mixtures used in this study. The optical birefringence at 530 nm (Δn), the sign of the dielectrical anisotropy ($\Delta\epsilon$) and the critical temperature (T_c) are provided by the manufacturer. The bandgap energy is estimated after the measurement of the UV absorption edge of the LC films.**

LC mixture	Δn	$\Delta\epsilon$	T_c	Bandgap energy
MLC2073	0.11	< 0	102°C	4.3 eV
MLC2132	0.25	> 0	114°C	3.2 eV
E7	0.22	> 0	58°C	3.2 eV

Spectral interferometry monitoring

In order to implement a real time monitoring of the film state and of the film optical thickness, the testing arm is inserted in a Mach-Zender interferometer (Fig. 1a). The pump pulse is thus recombined with a delayed replica, selected before the interaction with the LC film. A spectrometer (Avantes, 0.07 nm resolution) is employed to monitor the interferogram pattern. Spectral-domain interferometry combined with Fourier analysis is a powerful tool for metrology [22, 23], with numerous practical applications, such as optical index and/or group index, or phase response of metasurfaces measurements [24–27]. In practice, a Fourier Transform of each acquired spectrum is followed by temporal filtering in the Fourier space. Inverse Fourier Transform then provides the phase mismatch between the two arms of the interferometer. From the monitored phase, we can trace back the optical path variations in the testing arm.

The setup intrinsic stability is first tested. Fig. 2a shows the phase noise resulting from a 1s acquisition (acquisition period : 2 ms), with no film inserted in the beam path. The phase noise is about 50 mrad rms. The same measurement performed with and without film therefore provides an estimation of the film thickness, assuming an average refractive index of 1.6 [26, 28], with an error of $\simeq$ 10 nm. The statistical distribution of the thicknesses of some films realized for that study is shown in Fig. 2b, with an average value close to 100 nm.

Damage test procedure

Both 1-on-one and S-on-one test procedures have been implemented [29]. This choice is justified as follows: (i) 1-on-one provides LIDT measurements without the fatigue effects or heat build-up influence in the LC film and therefore to link LIDT with the medium bandgap, (ii) S-on-one procedure is closer to experimental conditions for most applications. Considering the wide scope of applications of LC-SLMs for laser beam shaping, the repetition rate is tuned between 100 Hz and 1 MHz. The experimental protocol is the following:

1. Renew the film with the method described in ,
2. Wait for a few tens of seconds for the film to reach a steady mechanical state (no macroscopic moves observable with the endoscope),
3. Exposure:
   (a) For S-on-one procedure: open the shutter, acquire 2000 consecutive spectra (acquisition period: 2 ms), close the shutter after 4 seconds of exposure,
   (b) For single-shot acquisition: open the shutter, send a single shot to the LC film, close the shutter.
4. Damage detection: measurement of the optical thickness of the film by spectral-domain interferometry

The search is then binary: after each exposure, the laser energy is decreased if damage is observed and, conversely, increased if no damage occurs.

Damage detection

LIDT is usually defined as a any change visible under a microscope with at least $\times 100$ magnification. The damage detection can occur in real-time or after exposure. In our study, the damage detection is rather simple and corresponds to the LC film breakdown. Damage detection is thus *in situ* and in real-time. Fig. 2c shows a typical spectrogram registered during exposure and breakdown of a LC film. In that case, breakdown occurs $\simeq 150$ ms after opening the shutter and is visible as a sudden phase shift of the interference fringes. The phase extracted from the spectrogram is plotted in Fig. 2d. We clearly see a progressive phase change followed by a sudden drop. This drop corresponds to the breakdown of the film. We explain the preceding phase decrease as a change of the inner film thickness under the effect of laser radiation. This can be explained as follows. The laser absorption, whatever its origin, and the resulting energy transfer, introduces a modification of the surface tension of the film. According to the Marangoni mechanism, this forces convection movements in the film which reduces the inner thickness until it breaks. Marangoni effect has been observed in LC under thermal changes due to laser absorption in LC films deposited on a solid substrate [30].

Statistical analysis

As thin films are intrinsically fragile, random breakdowns might happen as well. In order to improve the repeatability and determinism of the study, measurements are performed on over more than 600 samples for the entire experiment. For each experimental configuration (repetition rate or pulse duration) and for each of the three LC mixtures, we can organize the data as breakdown probability (1 = breakdown, 0 = no breakdown) as a function of laser fluence (Fig. 3) and apply a sigmoid fit function. The steeper the fit function is, the more deterministic the measurement of the LIDT is [31]. The fit then provides the LIDT value defined as the fluence for a damage probability of 0.5. Error bars correspond to damage probability of 0.1 and 0.9. An illustration of this method is shown in Fig. 3. The low deterministic nature of the damage can be explained by several factors: the soft matter nature of the sample, the film fragility and the laser pulse duration [31].

EXPERIMENTAL RESULTS

Laser repetition rate influence

The measured LIDT as a function of the laser repetition rate is shown in Fig. 4. All these measurements are performed using the same pulse length of 180 fs. We can clearly see here the decreasing of the LIDT when the repetition rate increases. The highest handled fluence for each mixture is measured with the lowest repetition rate (100 Hz) and is around 0.45 J/cm^2. This value is decreased by a factor of 10 for the highest repetition rate (1 MHz). For this repetition rate, the film has less time to cool down between each pulse. It thus indicates that thermal effects occur and have a significant influence on LCs LIDT. The first thing to take into account is our acquisition method. The exposure time is the same regardless of the repetition rate, thus, a fatigue effect under incubation or multiple shots accelerates the aging of the film. Furthermore, for the high repetition rates, thermal relaxation differs significantly [32]. Thus, thermal macroscopic processes, like the Marangoni effect, are favoured and conduct to an earlier breakdown. All three mixtures show the same trend: an abrupt change of the damage fluence between 100 Hz and 5kHz, followed by a much weaker dependence up to 1 MHz, nearly a plateau. Between 100 Hz and 5 kHz repetition rate, one can note that

the three mixtures exhibit different behavior. A LIDT abrupt change occurs between 100 Hz and 1 kHz for E7, and between 1 kHz and 5 kHz for MLC2073. Meanwhile, the LIDT decrease is nearly linear for MLC2132. These findings demonstrate the importance of thermal accumulation in the damage mechanism of liquid crystals. LCs are actually characterized by a low thermal conductivity ($0.13\,\mathrm{Wm^{-1}K^{-1}}$ for E7 [33]), which limits thermal relaxation. The differences observed between the three mixtures at 1kHz might thus originate from changes in thermal conductivity. Even in this regime where thermal dissipation is important, no influence of the film thickness on the LIDT value has been found.

The influence of the pulse duration is then investigated, by tuning the laser compression to cover the 180 fs- 1800 fs range. MLC2132 is used for that study, and the laser repetition rate is fixed to 20 kHz and 100 Hz. The results are shown in Fig. 5. At 20 kHz, the pulse duration has no effect on the LIDT, suggesting that the heating is induced by linear absorption. Although the LC is transparent at 1030 nm, impurities and/or small changes of the molecular structure may be associated with residual absorption. Such impurities might also be the cause of the differences observed between the mixtures. At 100 Hz, a weak linear dependence with pulse duration emerges, indicating that the dominant mechanism of damage is likely to be different. This is further investigated in the next section.

In most of LC devices, a thin film of polyvinyl alcohol (PVA) is spin-coated on the confinement substrate and then rubbed to anchor the molecules in a given direction. In order to determine whether this anchoring layer may reduce the LIDT of these devices by comparison with the LC itself, the same measurement protocol is applied to PVA films, for two repetition rates. The solution consists in 4% PVA diluted in pure water, deposited in a manner analogous to the LC. The results appear in Table II. The determined LIDT values are very close to those recorded for E7. Thus, PVA is not a critical issue for most of LC-based laser shapers. However, for mixtures with higher LIDT (saturated compounds or glassy LC mixtures [19]), alternative anchoring techniques [34] might be preferred .

TABLE II. **LIDT measurements for PVA and E7 films.**

Repetition rate	PVA LIDT (J/cm^2)	E7 LIDT (J/cm^2)
5 kHz	0.16±0.01	0.09±0.01
20 kHz	0.09±0.01	0.07±0.01

Single shot study

LIDT results with single-shot exposure are shown in Fig. 6 and summarized in Table III. The measured LIDT are more than twice higher than for pulse trains. All of the three mixtures have a damage threshold higher than 1 J/cm^2. Furthermore, it is found that LIDT for MLC2132 is nearly identical, while MLC2073 LIDT is 1.5 times higher. This is in good agreement with their bandgap energy ratio (Table I) and, following [19], it confirms that mixtures with higher bandgap present higher resistance to laser damage for single-shot exposure. Besides, MLC2132 has a more deterministic behavior than the two other mixtures, which is not understood at this stage. As a first conclusion, the viability of LC for intense femtosecond laser applications is assessed. In addition, the comparison with the substrates typically employed to develop LC devices, whether they are electro-optically or thermo-optically addressed, confirm that the metallic or the conductive layers are the limiting factor for LIDT in the femtosecond regime (Table III).

TABLE III. **LIDT measurement with a single shot exposure. Values reported in the literature for LC devices substrates is shown for comparison (* refers to measurements performed in the ns regime).**

LC mixture	LIDT (J/cm^2)	Substrate	LIDT (J/cm^2)
MLC2073	1.79 ± 0.28	SiO2	3.5 [29]
MLC2132	1.12 ± 0.07	Au	0.6 [35]
E7	1.13 ± 0.21	ITO	0.47* [14]
		GaN	1.67* [14]

Single-shot LIDT dependence on pulse duration is then assessed. MLC2132 is again selected for that parametric study, because of the more deterministic nature of its LIDT measurement (Fig. 6). The results are shown in Fig. 5. The single-shot LIDT dependence on the pulse duration is not constant anymore. Here the dependence can be fitted by a power law of the pulse duration (τ), following $F_{th} = \tau^x$ with $x \simeq 0.2$. This suggests, that in this regime, the breakdown is due to intrinsic properties of the material (not its impurities nor its defaults) and particularly electronic mechanisms. For dielectrics in the sub-picosecond regime, some phenomenological models attribute the pulse duration dependence to the interplay of multiphoton ionization, impact ionization, and subpicosecond electron decay out of the conduction band [36–39]. The power exponent x of the observed dependence of the breakdown threshold on pulse duration depends on the balance between these mechanisms. Additional investigations conducted at shorter pulse duration will be needed to provide a better understanding of all the processes involved here.

We underline that our measurements nicely complete the study reported in [19], in which the minimum laser pulse duration was 600 fs. Values reported for E7, the common mixture to both studies, are in overall good agreement. However, the data corresponding to long pulse length cannot be accurately compared, because of different testing material (MLC2132 versus other mixtures in [19]), different testing sample (freely-suspended films versus LC cell which could undergone self-focusing)

and different damage criterion (thin films breakdown versus LC cell damage observed under a microscope).

Finally, as demonstrated by previous works, a linear dependence is expected between the bandgap of the dielectrics and the single-shot LIDT measurement. Here we find that LCs exhibit a slightly higher damage threshold than materials of comparable bandgap. For instance, Ta_2O_5, TiO_2 and Nb_2O_5 are characterized by a single shot damage threshold between 0.5 and 0.7 J/cm^2 for a bandgap energy between 3.3 eV and 3.8 eV [29, 37]. A potential explanation to this discrepancy could be the criterion used here to define the optical damage (film breakdown), which differs significantively from the one used for bulk media.

CONCLUSION

To conclude, we have studied laser-induced breakdown of thin nematic liquid crystal films, in the femtosecond regime. We have proposed an original experimental approach, relying on three main features. (*i*) The samples were freely-suspended nematic films, with a reliable thickness as low as 100 nm. (*ii*) We have implemented spectral interferometry to monitor *in situ* and in real time the films optical thickness with a 10 nm resolution. The method fidelity opens some perspectives to study convection motion in soft matter films. (*iii*) A statistical approach over more than 600 films, for the entire experiment, has shown the low deterministic character of laser-induced breakdown of such materials.

The multi-parameter study (fluence, repetition rate, pulse duration and LC mixtures) has shown that two regimes can be distinguished for LC breakdown. In the single-shot regime, breakdown seems dominated by the usual ionization processes in dielectrics and LIDT is above 1 J/cm^2 for the three mixtures investigated here. Meanwhile, exposure to high repetition rate pulses train (¿100 Hz) indicate a breakdown dominated by thermal accumulation due to residual linear absorption. At 1kHz, measured LIDT is $\simeq 0.1$ J/cm^2 for the widely used E7.

The three nematic mixtures investigated here (E7, MLC2132, MLC2073, from Merck) have shown similar behavior in this multi-parameter study. However, some differences between them have been pointed out. (*i*) The highest single-shot LIDT is assessed for the mixture featuring the highest bandgap energy. Therefore, it indicates that the single-shot LIDT is governed by the molecular structure itself. (*ii*) The deterministic character of LIDT varies from one mixture to another, as well as the transition between the two regimes mentioned earlier (*iii*). The latter observation can be attributed to different thermal properties and/or different causes of residual linear absorption.

According to both 1-on-one and S-on-one test procedures, the LIDT values strengthen the use of nematics as innovative phase shapers for intense and/or ultrashort laser systems, or as nonlinear materials in the femtosecond regime. Forthcoming studies will focus on the study of LC damage in the sub-50 fs regime and under other excitation wavelengths.

FUNDING

The authors thank the Agence Nationale de la Recherche France (Grant: ANR-19-CE30-0006-01, UNLOC),the European Regional Development Fund (OPTIMAL) for financial support and Agence Nationale de la Recherche et Technologie (ANRT, 2019/0660).

ACKNOWLEDGMENTS

The authors thank Matthieu Bellec for the loan of the *xyz* platform.

DISCLOSURES

The authors declare no conflicts of interest.

DATA AVAILABILITY STATEMENT

Data underlying the results presented in this paper are not publicly available at this time but may be obtained from the authors upon reasonable request.

[1] D.-K. Yang, S.-T. Wu, *Fundamentals of liquid crystal devices*, Wiley (2012).
[2] I.-C. Khoo, *Liquid crystals, Physical properties and nonlinear optical phenomena*, Wiley (1995).
[3] *Spatial Light Modulator Technology: Materials, Devices, and Applications*, ed. Efron (1995)
[4] G. D. Love, *Adaptive Optics Engineering Handbook*, ed. CRC Press (1999)
[5] D. J. Cho, S. T. Thurman, J. T. Donner, G. M. Morris , "Characteristics of a 128×128 liquid-crystal spatial light modulator for wave-front generation", Opt. Lett. **23,** 969 (1998).
[6] S.-T. Wu, U. Efron, L. D. Hess, "Birefringence measurements of liquid crystals", App. Opt. **23,** 3911 (1984).
[7] T. Kuki, H. Fujikake, T. Nomoto, Y. Utsumi, "Design of a Microwave Variable Delay Line Using Liquid Crystal, and a Study of Its Insertion Loss", Electron. Comm. in Japan **85,** 90 (2002).
[8] C.-S. Yang, T.-T. Tang, P.-H. Chen, R.-P. Pan, P. Yu, C.-L. Pan, "Voltage-controlled liquid-crystal terahertz phase shifter with indium-tin-oxide nanowhiskers as transparent electrodes", Opt. Lett. **39,** 2511 (2014).
[9] C. Dorrer, S. K.-H. Wei, P. Leung, M. Vargas, K. Wegman, J. Boulé, Z. Zhao, K. L. Marshall, S. H. Chen, "High-damage-threshold static laser beam shaping using

optically patterned liquid-crystal devices", Opt. Lett. **36**, 4035 (2011).

[10] A. Jullien, U. Bortolozzo, S. Grabielle, J.-P. Huignard, N. Forget, S. Residori, "Continuously tunable femtosecond delay-line based on liquid crystal cells", Opt. Exp. **24,** 14483, (2016).

[11] Y. Liu, H. Liang, C-W. Chen, X. Xie, W. Hu, P. Chen, J. Wen, J. Zhou, T.-H. Lin, I. C. Khoo, "Ultrafast switching of optical singularity eigenstates with compact integrable liquid crystal structures", Opt. Exp., **26,** 28818, (2018).

[12] P. S. Salter, M. J. Booth, "Adaptive optics in laser processing", Light: Science and Applications, **8,** 110, (2019).

[13] V. M. di Pietro, A. Jullien, U. Bortolozzo, N. Forget, S. Residori, "Thermally-induced nonlinear spatial shaping of infrared femtosecond pulses in nematic liquid crystals", Laser Phys. Lett. **16,** 015301, (2018).

[14] Z. Xing, W. Fan, D. Huang, H. Cheng, G. Xia, "High laser damage threshold liquid crystal optical switch based on a gallium nitride transparent electrode", Opt. Lett. **45,** 3537, (2020).

[15] K. L. Marshall, T. Z. Kosc, M. Ordway, L. Guo, M. Johnston, A. Callahan, H. Carder, "Optically-addressable liquid crystal laser beam shapers employing photoalignment layer materials and technologies", Liquid Crystals XXII, International Society for Optics and Photonics (2018).

[16] V.M. di Pietro, S. Bux, N. Forget, A. Jullien, "Phase-only pulse shaper for multi-octave light sources", Opt. Lett., **45,**, 543-546, (2020).

[17] S. D. Jacobs, K. A. Cerqua, K. L. Marshall, A. Schmid, M. J. Guardalben, K. J. Skerrett, "Liquid-crystal laser optics: design, fabrication, and performance", Journ. of Opt. Soc. Am. B, **5,**, 1962 (1988).

[18] Z. Raszewski, W. Piecek, L. Jaroszewicz, L. Soms, J. Marczak, E. Nowinowski-Kruszelnicki, P. Perkowski, J. Kedzierski, E. Miszczyk, M. Olifierczuk, P. Morawiak, R. Mazur, "Laser damage resistant nematic liquid crystal cell", Journ. of Applied phsyics, **114,**, 053104 (2013).

[19] T. Z. Kosc, A. A. Kozlov, S. Papernov, K. R. P. Kafka, K. L. Marshall, S. G. Demos, "Investigation of parameters governing damage resistance of nematic liquid crystals for high- power or peak-intensity laser applications", Scientific Reports, **9,** 16435, (2019).

[20] P. L. Poole, C. D. Andereck, D. W. Schumacher, R. L. Daskalova, S. Feister, K. M. George, C. Willis, K. U. Akli, E. A. Chowdhury, "Liquid crystal films as on-demand, variable thickness (50–5000 nm) targets for intense lasers", Physics of Plasmas, **21,** 063109, (2014).

[21] P. L. Poole, C. Willis, G. E. Cochran, R. T. Hanna, C. D. Andereck, D. W. Schumacher, "Moderate repetition rate ultra-intense laser targets and optics using variable thickness liquid crystal films", App. Phys. Lett., **109,** 151109, (2016).

[22] L. Lepetit, G. Cheriaux, M. Joffre, "Linear techniques of phase measurement by femtosecond spectral interferometry for applications in spectroscopy", J. Opt. Soc. Am. B, **12**, 2467-2474, (1995).

[23] A. Borzsonyi, A. P. Kovács, K. Osvay, "What We Can Learn about Ultrashort Pulses by Linear Optical Methods", App. Sc., **3**, 515, (2013).

[24] W. V. Sorin, D. F. Gray, "Simultaneous Thickness and Group Index Measurement Using Optical Low- Coherence Reflectometry", IEEE Phot. Techn. Lett., **4**, 105, (1992).

[25] S. Rivet, A. Bradu, F. Bairstow, H. Forrière, A. Podoleanu, "Group refractive index and group velocity dispersion measurement by complex master slave interferometry", Opt. Express **26,**, 21831, (2018).

[26] V. M. Di Pietro, A. Jullien, "Broadband Spectral Domain Interferometry for Optical Characterization of Nematic Liquid Crystals", App. Sc. **10,**, 4720, (2020).

[27] L. Michaeli, D. Ben Haim, M. Sharma, H. Sucowski, T. Ellenbogen, "Spectral interferometric microscopy for fast and broadband phase characterization", Adv. Opt. Mat., 2000326 (2020).

[28] J. Li, C. H. Wen, S. Gauza, R. Lu, S. T. Wu, "Refractive Indices of Liquid Crystals for Display Applications", J. Display Technol. **1**, 51 (2005).

[29] B. Mangote, L. Gallais, M. Zerrad, F. Lemarchand, L. H. Gao, M. Commandré, M. Lequime, "A high accuracy femto-/picosecond laser damage test facility dedicated to the study of optical thin films", Rev. Sci. Inst., **83,** 013109 (2012).

[30] J. B. Poursamad, F. B. Jahanbakhsh, M. Asadpour, A. Phirouznia, "The Marangoni effect in nematic liquid crystals due to a Gaussian light beam absorption", Journ. of Mol. Liquids, **186,** 23 (2013).

[31] N. Sanner, O. Uteza, B. Chimier, M. Sentis, P. Lassonde, F. Legare, J. C. Kieffer, "Toward determinism in surface damaging of dielectrics using few-cycle laser pulses", App. Phys. Lett., **96,** 071111 (2010).

[32] B. J. Nagy, L. Gallais, L. Vámos, D. Oszetzky, P. Rácz, P. Dombi, "Direct comparison of kilohertz- and megahertz-repetition-rate femtosecond damage threshold", Opt. Lett., **40,** 2525 (2015).

[33] X. He, X. Wang, L. Wu, Q. Tan, M. Li, J. Shang, S. Wu, Z. Huang, "Theoretical modeling on the laser induced effect of liquid crystal optical phased beam steering", Opt. Comm., **382,** 437 (2017).

[34] I. A. Pavlov, A. S. Rybak, A. M. Dobrovolskiy, V. M. Kadan, I. V. Blonskiy, Z. I. Kazantseva, I. A. Gvozdovskyy, "High-quality alignment of nematic liquid crystals using periodic nanostructures created by nonlinear laser lithography", Journal of Molecular Liquids, **267,** 212 (2018).

[35] P. Poole, S. Trendafilov, G. Shvets, D. Smith, Enam Chowdhury, "Femtosecond laser damage threshold of pulse compression gratings for petawatt scale laser systems", Opt. Express, **21,** 26341 (2013).

[36] B. C. Stuart, M. D. feit, S. Herman, A. M. Rubenchik, B. W. Shore, M. D. Perry, "Nanosecond to femtosecond laser induced breakdown in dielectrics", Phys. Rev. B, **53,** 1749 (1996).

[37] M. Mero, J. Liu, W. Rudolph, D. Ristau, K. Starke, "Scaling laws of femtosecond laser pulse induced breakdown in oxide films", Phys. Rev. B, **71,** 115109 (2005).

[38] M. Lenzner, "Femtosecond laser-induced damage of dielectrics", International Journal of Modern Physics B, **13,** 1559 (1999).

[39] J. Jasapara, A. V. V. Nampoothiri, W. Rudolph, D. Ristau, K. Starke, "Femtosecond laser pulse induced breakdown in dielectric thin films", Phys. Rev. B, **63,** 045117 (2001).

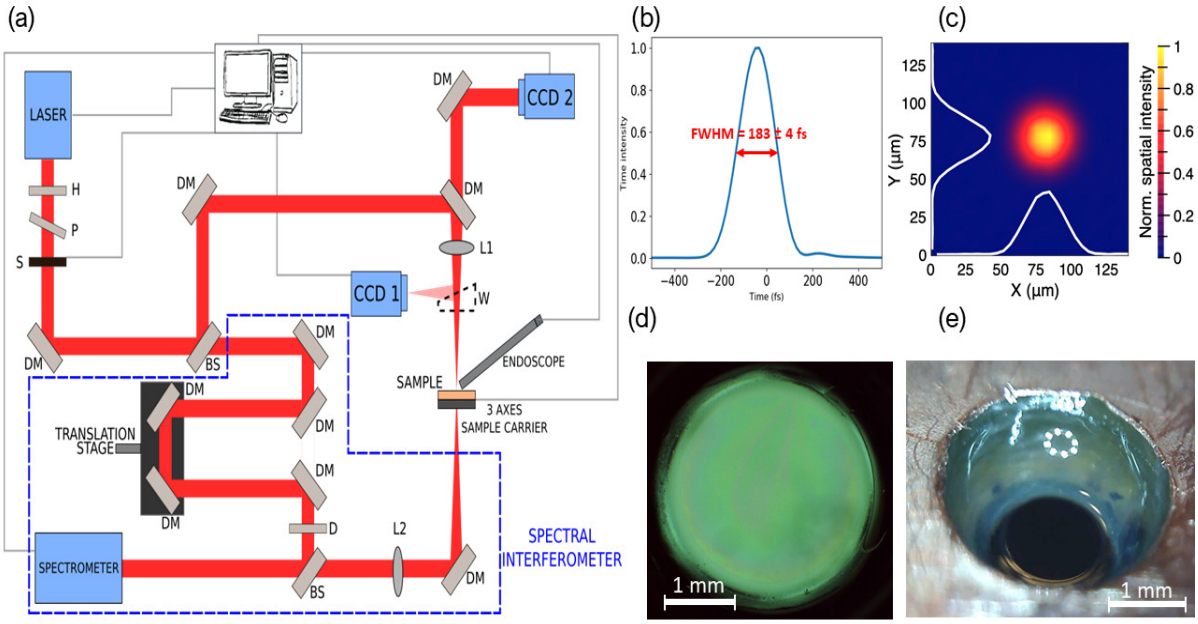

FIG. 1. (a) Experimental setup for LIDT measurements. H: half wave plate, P: polarizer, DM: dielectric mirror, BS: beam splitter, W: removable wedge, S: mechanical shutter, D: variable density, L1: focusing lens f = 150 mm, L2: focusing lens f = 200 mm, CCD 1 : camera used for the measurement of the spot size at focus, CCD 2 : camera used for aligning the laser spot on the sample. (b) Pulse temporal intensity and duration reconstructed from the FROG measurement. (c) Laser focused spot visualized on CCD1. (d) A LC film as observed by optical microscopy (transmission mode, unpolarized light). The copper plate is regularly cleaned with ethanol. With the microscope, we haven't noticed any visible impurity added between successive films. (e) A LC film as observed *in situ* by the endoscope (the circle of white is the reflection of the endoscope light).

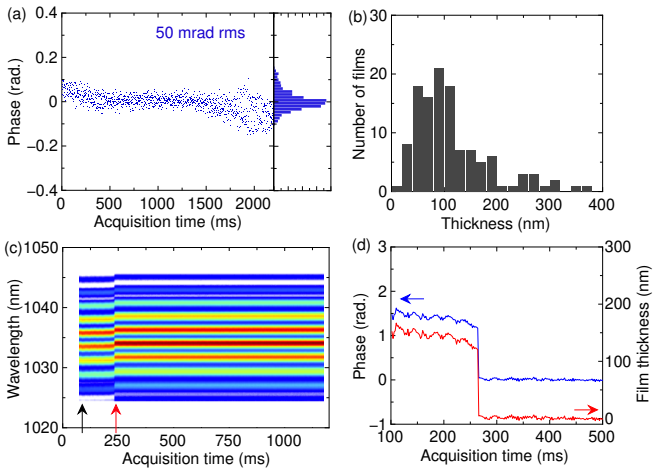

FIG. 2. (a) Measured phase stability of the interferometer as a function of acquisition time. The relative group delay between the two interfering pulses is 1.6 ps. There is no sample for this acquisition. The phase noise is 50 mrad rms over 1s. (b) Distribution of the thickness of the produced films, all mixtures combined. (c) Typical spectrogram registered during laser exposure of a thin film of MLC2132. The black arrow indicates the beginning of laser exposure, the red arrow underlines the film breakdown, visible as a sudden phase shift of the interference pattern and an increase of the fringes contrast (d) Phase variations (blue) retrieved after numerical treatment on (c), zoomed in on the breaking of the LC film. The film relative thickness (red) is deduced by assuming an average optical index of 1.6 [26, 28].

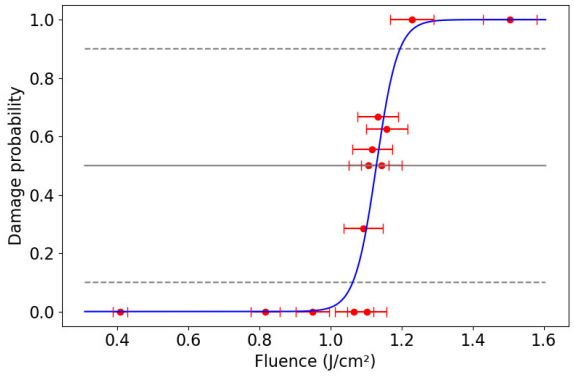

FIG. 3. Laser damage probability (1 = breakdown, 0 = no breakdown) in red for several fluences and sigmoid fit (in blue) of the data in the single shot regime and on MLC2132. The dashed grey lines correspond to the 10% uncertainty limit and the plain line corresponds to the LIDT. From this plot comes the LIDT value for MLC2132 in the single shot regime : 1.12±0.07 J/cm^2 (discussed in section).

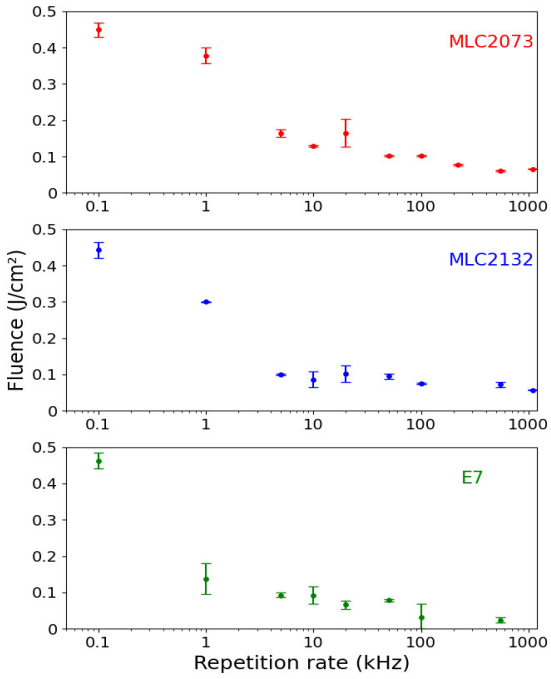

FIG. 4. Laser damage thresholds measured on 3 LC mixtures with laser repetition rate ranging between 100 Hz and 1 MHz. The laser pulse duration is (183±4) fs.

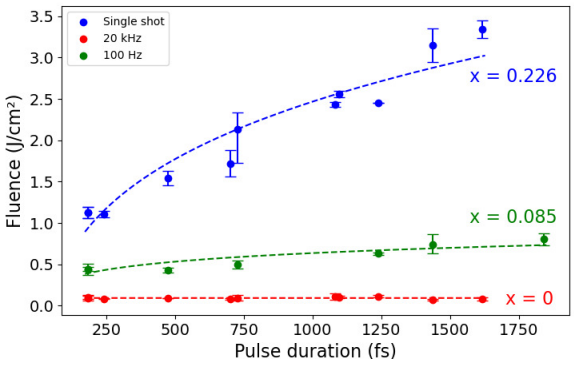

FIG. 5. Laser damage thresholds measured as a function of the pulse duration for two different repetition rates and the single-shot regime. The LC mixture is MLC2132. The dashed lines correspond to a $F_{th} = \tau^x$ fit, with F_{th} the LIDT, τ the pulse duration and x the fitting parameter indicated on the figure for each repetition rate.

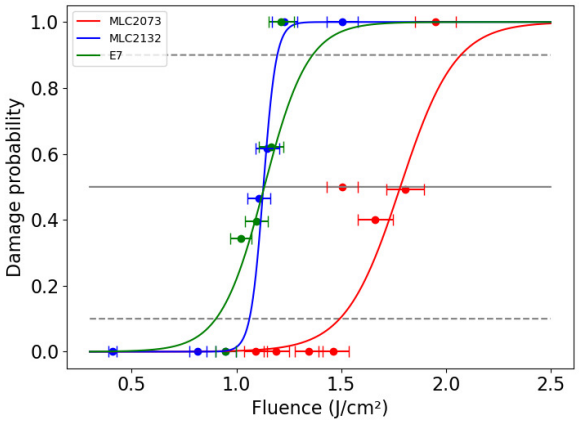

FIG. 6. Laser damage probability as a function of the fluence in the single shot regime and sigmoid fit of the data. The results on the three different mixtures of LC are presented and LIDT values are shown in Table III.